The micro-arcsecond metrology testbed (MAM)

S. Shaklan, S. Azevedo, R. Bartos, A. Carlson, Y. Gursel, P. Halverson,
A. Kuhnert, Y. Lin, R. Savedra, E. Schmidtlin

Jet Propulsion Laboratory, California Institute of Technology
4800 Oak Grove Dr., M/S 306-388, Pasadena, CA 91109

ABSTRACT

The micro-arcsecond metrology testbed (MAM) is a high-precision long baseline interferometer inside a vibration-isolated vacuum tank. The instrument consists of an artificial star, a laser metrology system, and a single-baseline interferometer with a 1.8 m baseline and a 5 cm clear aperture. MAM's purpose is to demonstrate that the astrometric error budget specified for the Space Interferometry Mission can be met.

Keywords: Interferometry, Space Interferometry Mission, astrometry

1. INTRODUCTION

The Space Interferometry Mission (SIM) is currently a Phase A NASA project being developed at the Jet Propulsion Laboratory (JPL). Its primary mission is to perform high-precision astrometry of a large sample of galactic and extra-galactic objects. With its unprecedented 4 micro-arcsecond accuracy, SIM can detect thousands of extra-solar planets, measure the distance to the furthest stars in our galaxy, and calibrate cosmological distance beacons[1].

In parallel with the spacecraft and flight instrument design efforts, JPL is building several testbeds to develop the necessary technology required for a successful mission. This paper describes one of these testbeds, the Micro-Arcsecond Metrology Testbed. MAM is designed to demonstrate simultaneous high-precision laser metrology and white-light fringe measurements in a SIM-like interferometer. It will serve as a proving ground for both optical and thermal modeling. MAM is currently in the late design and early integration stages; a significant fraction of the interferometer and metrology hardware will be completed by the end of this year.

2. CONCEPTUAL DESIGN

An optical long-baseline interferometer determines the angle of a star relative to the baseline vector by measuring the phase delay of the white-light fringe pattern. Fringes are formed by combining the starlight entering the interferometer's two arms. SIM consists of three white-light interferometers that share the same baseline (plus a fourth for redundancy). One baseline is used to measure science targets while the other two simultaneously observe reference stars. The reference stars provide knowledge of the baseline orientation. A laser metrology system measures the baseline length. Thus, the baseline vector is determined from reference star and laser metrology measurements. Additionally, SIM has pointing and optical path control systems that are used to stabilize the interference pattern on a charged-coupled device (CCD) or an avalanche photo-diode (APD). The optical delay is measured with a laser metrology system that monitors the motion of the optical delay line relative to retro-reflectors that form the baseline endpoints. SIM's fundamental observables are stellar white-light fringe positions and laser-metrology path measurements.

MAM makes the same fundamental measurements as SIM. However, it has only one baseline. Instead of additional interferometers to provide knowledge of the baseline orientation, MAM uses supplemental laser metrology to monitor the positions of the baseline end-points relative to an artificial star. The laser metrology provides a "truth" measure of the white-light fringe delay that is compared to the measured white-light fringe delay. Like SIM, the MAM interferometer has pointing systems, optical path control systems, laser metrology, and fringe detectors. It operates in a vibration-isolated, thermally stable, vacuum tank so that its control system can stabilize fringes to the levels consistent with micro-arcsecond astrometry.

This allows MAM to investigate astrometric performance relative to a SIM-like error budget. Through controlled experiments, one can determine the sensitivity to optical aberrations, beam walk, field-of-regard, thermal gradients, etc.

Because it has a single baseline, MAM does not interrogate the entire SIM astrometric error budget. But the vast majority of error sources are related to a single baseline. The successful operation of MAM is an important milestone as we design, build, and test the SIM instrument.

In summary, MAM measures the position of a white-light fringe and compares the measurements to predictions derived from laser metrology. Though MAM may look like a simplified version of SIM, its astrometric performance is closely linked to its space-borne cousin.

MAM was conceived with another important goal, namely to serve as a proving ground for optical modeling tools. The development of high-precision models is crucial to designing and calibrating SIM. Experiments in a controlled environment, combined with detailed knowledge of the MAM optical elements, will allow us to refine our models and explore their robustness, dynamic range, and fidelity.

3. ARCHITECTURE

The MAM architecture is shown in Fig. 1. MAM consists of three major subsystems: interferometer, metrology system, and artificial star. The interferometer input optics, metrology system, and artificial star all lie in a plane. Each arm of the single-baseline interferometer contains a siderostat, fast steering mirror, delay line, and optics for separating light that is used to form interference fringes from light that is used for angle tracking. The combined beams from the two arms are detected by either a single-pixel APD or as dispersed fringes in a channeled spectrum on a CCD. This will be explained in some detail below, but see Carlson *et al*[2] for a complete description.

The metrology system consists of a stabilized Nd:YAG laser source, a heterodyne modulation system, optical beam launchers that measure the distance between corner-cubes, and phase detection electronics. See Dubovitsky *et al*[3] for a complete description of the laser source. Kuhnert *et al*[4] explain the metrology optics, detection and methodology. Schmidtlin *et al*[5] describe the multiple-face corner cubes.

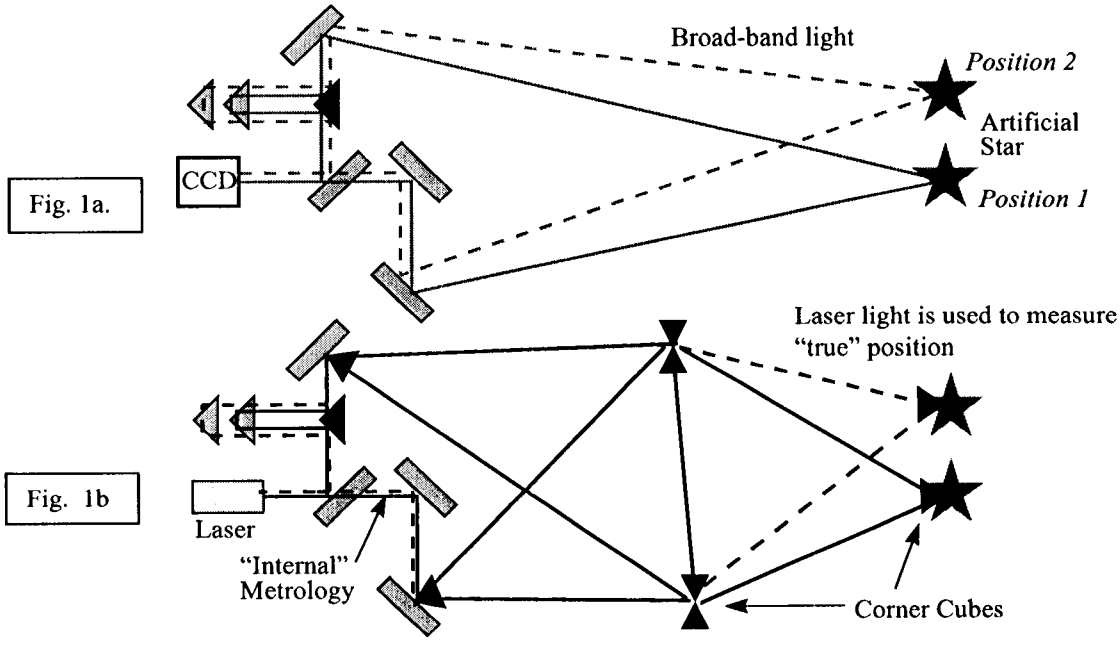

Figure 1. MAM architecture. Fig. 1a shows the starlight architecture: an artificial star illuminates a single baseline interferometer. Fig. 1b shows the metrology system. The artificial star is co-located with a corner cube. Heterodyne laser beams monitor the positions of the siderostats relative to the star.

The metrology system serves two purposes: "internal metrology" measures the distance between the beamsplitter and the siderostats. This determines how much the optical path changes as the delay line slews to track the artificial star. "External metrology" is the set of laser beams and corner cubes in the middle of fig. 1b. These form a two-dimensional truss, the lengths of which are insensitive to first order to out-of-plane motions. The siderostats are on one side of the truss while the artificial star is at the other side. The 7 external metrology measurements are combined to determine how the artificial star moves with respect to the siderostats. Thus the "truth" measure discussed above is derived by combining the internal and external metrology measurements. These measurements allow one to compute the star-to-beamsplitter optical path. If the experiment is functioning properly, the computed optical path agrees with the measured white-light optical path to levels commensurate with micro-arcsecond astrometry.

The artificial star is a single-mode fiber optic placed close to the optical vertex of a corner-cube. The light source is an intensity-stabilized quartz-halogen lamp. A single-mode (SM) fiber is used because it is a virtually perfect source of spherical waves. The lateral emanation point of the waves is independent of wavelength, while the axial depth dependence is negligible. The corner cube is used to retro-reflect the metrology beams. The artificial star assembly is placed on a rotation/translation stage (the purpose for the rotation stage is described in Sect. 4.3). As the star is translated, the metrology beams, siderostats, and delay lines all track its motion.

The SM fiber beam spreads with a numerical aperture of about 0.1. This is the main driver behind both the long dimension of the vacuum tank (45 ft end-to-end) and the length of the baseline (1.8 m). A fiber with higher numerical aperture would facilitate a shorter, stiffer, and less expensive tank. But it would exacerbate errors related to finite wavefront curvature and absolute laser metrology accuracy (see Sect V).

It is important to note that there are no optics between the artificial star and the interferometer. A conventional optical system to collimate the beams over a 1.8 m baseline would typically introduce 1% distortion. For a 5° field-of-regard, the resulting 180 arcseconds of distortion is 7 orders of magnitude larger than our desired measurement accuracy. It would be virtually impossible to calibrate to this level. Another possibility is to build two back-to-back interferometers. This could eliminate the distortion problem but it could potentially hide important errors because the source and the detector are both similar instruments.

4. HARDWARE

4.1 Vacuum system

MAM is designed to provide a quiet, isolated, thermally stable environment for interferometric experimentation. The nominal vacuum pressure required is ~ 10^{-4} Torr. This is driven mainly by the need to eliminate piezo-electric transducer (PZT) arcing, since a vacuum of 10^{-3} Torr would be sufficient for optical path stability and suppression of thermal convection. The thermal time constant desired is ~ 12 hours. This is driven by the time required to perform a multi-field-angle experiment. Ambient floor motion is nominally < 1 micron r.m.s. below 1 Hz, < 0.1 micron r.m.s. between 1-10 Hz, and < 10 nm above 10 Hz. Note that a lateral motion of 1 nm between the artificial star and the interferometer is equivalent to 20 micro-arcseconds. Thus the isolation system and thermal control are crucial for surpressing background astrometric disturbances.

The MAM vacuum chamber (fig. 2) is a 96 inch diameter by 480 inch long cylinder that was built by Howard Fabrication Inc. The vacuum chamber skin is 0.25 inch thick stainless steel. External ribs were placed every 30 inches along the length of the chamber to prevent buckling of the walls and raise the natural frequency of the local modes in the chamber walls above 40 Hz. The ribs are 5 inches deep by 0.5 inches wide and are fabricated from A36 steel. A total of 28 DN250-CF-F Conflat flanges were installed on the chamber to provide vacuum pump connections, view ports, fiber optic feed-throughs, and electrical feed-throughs. The entire chamber is mounted on two cradles that are separated by 270 inches. Each cradle is attached to the chamber using 2.5 inch diameter A36 rods configured to provide a kinematic flexure type mount to the chamber. The entire vacuum chamber is wrapped in ten layers of 5/16 inch thick aluminum foil face bubble wrap insulation to provide thermal stability inside the chamber. The vacuum chamber has a door at each end of the chamber for installing and removing equipment.

Two mounting rails with a pre-drilled bolt pattern are welded inside the chamber. Three 6 x 4 x 1 ft. optical tables will be installed inside the chamber. Each table will be mounted on a table mount that is attached to one of the internal rail mounting locations. The table mounts are a welded aluminum box tube structure. Rubber pads fabricated from RTV 615 will be

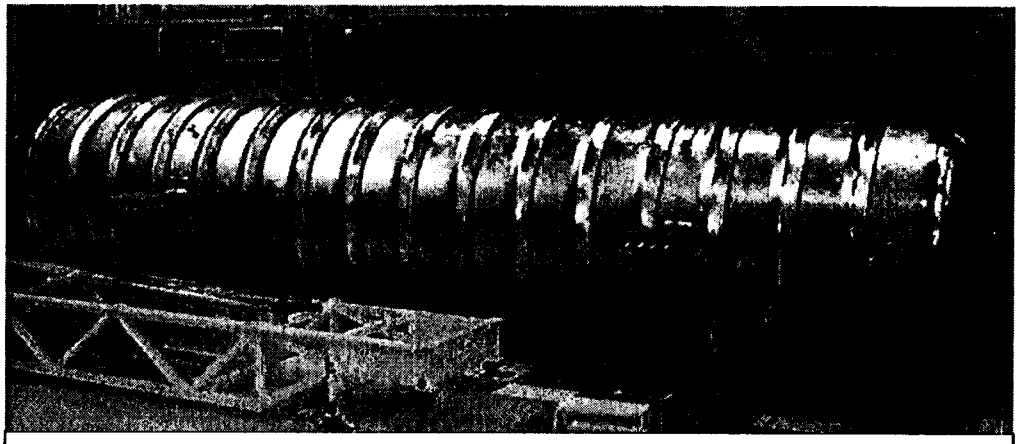

Figure 2. The MAM vacuum chamber is located in the Spacecraft Assembly Facility in Hi-Bay 1. This is a class 100,000 clean room.

placed between the table mounts and the optical tables to provide additional vibration isolation above 10 Hz between the tank and tables.

The empty chamber as fabricated weighs approximately 34000 pounds including the two cradles. When loaded with the optical tables and test equipment the total weight of the chamber is expected to be approximately 38000 pounds.

The vacuum pumping system is illustrated in fig. 3. The roughing pump is a Balzers model no. DUO-250A dual stage rotary vane pump. This pump has a nominal volume flow rate of 320 m^3 hr^{-1}, and is capable of achieving a final pressure < 1 mTorr. It is located in a small shed outside the high bay and is connected to the chamber by a 4" diameter line. For vibration isolation, the line contains a 12 ft. long bellows flex line between the gate valve and the roughing pump line. A magnetically-suspended-bearing Balzers turbo molecular drag pump sits on the vacuum chamber and is backed by a rotary pump (UNO-035D) located in the shed. The turbo pump kicks in when the pressure reaches 0.3 Torr. The final operating pressure of 10^{-4} Torr should be attained ~ 3-4 hours later. The entire pump-down time is expected to be < 8 hours.

4.2 Isolation system

The entire chamber is mounted on air springs to provide vibration isolation during the experiments. The MAM vacuum chamber is mounted on four Firestone Airmount Isolators Model # 19T19L-11 functioning at an 18 inch operating height. Each of the isolators is mounted and directly coupled to an external air reservoir with a 4275 cu. in. volume to lower the natural frequency of the system to 1 Hz. The reservoir is attached to the building foundation and the airmounts are attached to the cradles at the same elevation as the centerline of the chamber to provide a stable mounting. The natural frequency of the chamber mounted on the isolators is expected to be approximately 0.5 Hz.

4.3 Artificial star

The artificial star is a standard circular-core SM fiber with a cutoff wavelength λ_c=600 nm. The fiber is illuminated with an intensity stabilized, unpolarized quartz-halogen lamp. The tails of the near-Gaussian beam emerging from the fiber illuminate the interferometer located 10 m away. Even though the 1.8 m baseline partially resolves the core of the fiber, the single-mode source appears to be completely unresolved for $\lambda > \lambda_c$; fringe visibility in the ideal case is unity except for a negligible reduction due to the intensity gradient across the apertures. For shorter wavelengths, the interferometer resolves the multiple-modes. Light below 600 nm is separated by dichroic filters in the interferometer optical train (see below) to be used for angle tracking. The multi-mode character of the light is expected to result in < 10^{-7} radian centroiding errors, roughly 1/50 of the single-arm Airy pattern full-width half maximum (FWHM). The differential centroiding errors between the two arms should be even smaller.

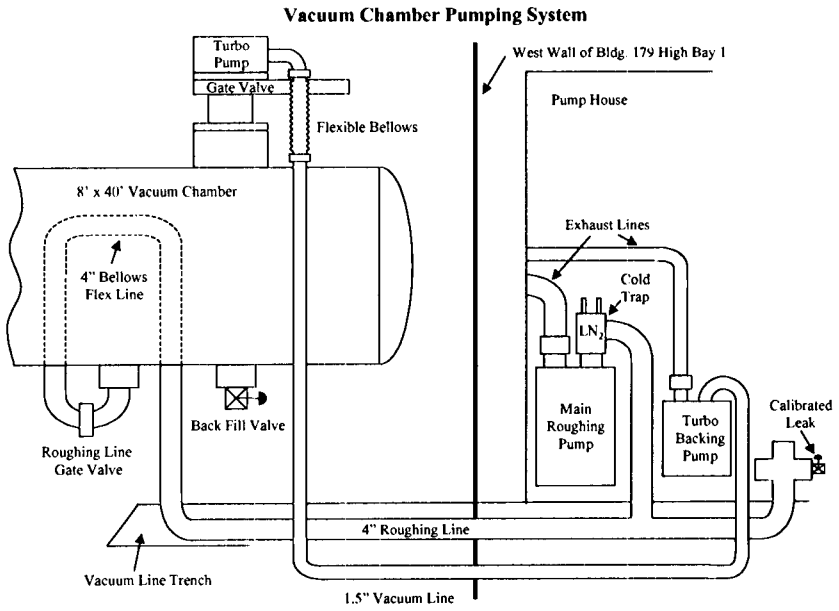

Figure 3. The MAM vacuum system. The roughing pump and turbo backing pump are located in a separate building on isolation pads.

The fiber is positioned at the optical vertex of an open-faced corner cube (fig. 4). The cube is constructed in the standard way, with three overlapping ULE flats placed at right angles. The measured gaps between the surfaces are < 50 microns. The vertex of the cube has been ground normal to the cube's axis of symmetry so that a hole ~ 100 microns in diameter is left at the vertex. A 25 mm long cylinder with a 1.08 mm diameter core-drilled hole is bonded to the ground section, forming a guide for the fiber and a convenient mounting fixture. The fiber is bonded with UV curing epoxy inside a fused silica tube with a 140 micron inner diameter and a 1.0 mm outer diameter. This tube is placed inside the ULE cylinder and positioned under a microscope so that the fiber appears at the optical vertex.

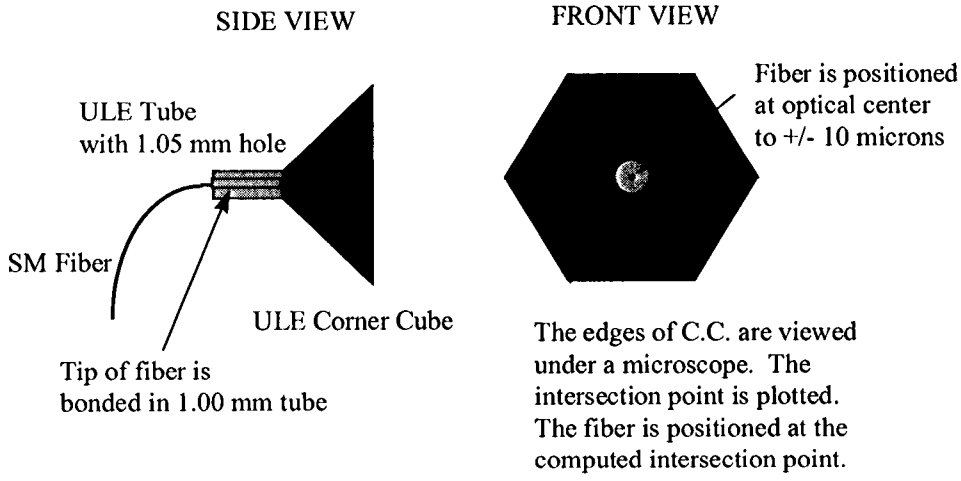

Figure 4. Conceptual description of the artificial star.

The optical vertex is determined using the following procedure: employing a microscope encoded on 3 axes with repeatable micron accuracy transducers, the regions around the interfaces (gaps) are determined by focusing on a piece of dust, a minute scratch, or an obvious feature at the gap. The microscope is then repositioned to the reflection of the object formed by the adjacent glass. Pairs of points are observed in this way along the gap and the central points are computed. This is repeated for the remaining two gaps. Since all of the observed features are located on (or within a micron or two) of the surfaces, each line represents a close approximation to the optical intersection of the surfaces. A least-squares fit is performed for each line, then the point of closest intersection is analytically computed. This point is the optical vertex of the corner cube. Preliminary results show a repeatability of < 10 microns for determining the intersection of the lines. The microscope is commanded to the vertex position, then the fiber/tube assembly is manipulated until the fiber tip appears in-focus at the center of the microscope field-of-view. The assembly is then glued into place using UV curing epoxy.

The completed assembly is placed in a rotation stage mounted on a translation stage. The rotation stage allows us to position the fiber directly above the corner cube vertex (out-of-plane) so that there is a negligible lateral offset between them. This is required because a lateral offset of even a few microns leads to significant angular errors between the interferometer and external metrology system as the star is scanned across the field-of-regard. The resulting ~10 micron out-of-plane vertical displacement of the fiber compared to the corner-cube vertex introduces < 10 picometers of optical path error in the metrology and white-light system.

4.4 Metrology

The metrology system consists of "internal" beam launchers and "external" beam launchers, corner cubes, a cat's-eye retro-reflector, and a stabilized laser source common to all of the metrology. A detailed description is given by Kuhnert *et al*[4]. Fig. 5 shows a block diagram of the metrology source from the laser through the frequency shifters, to the beamsplitter and the phase detector.

MAM uses two lasers operating at frequencies separated by 30 GHz. The measured phase difference between the two frequencies is used to create an artificial wavelength that allows us to make an absolute optical path measurement with a 5 micron accuracy and a 5 mm ambiguity. The ambiguity is removed using a theodolyte capable of surveying the MAM optics to ~ 0.1 mm. The lasers are non-planar ring oscillator Nd:YAGs manufactured by Lightwave Electronics Inc. The lasers deliver > 100 mW of continuous power, with typical linewidths of 5 kHz. The lasers are simultaneously locked to longitudinal modes of a ULE cavity[3], achieving a frequency stability < 10 Hz/sqrt(Hz) between 10 Hz and 10 kHz. This compares favorably to the required 450 Hz/sqrt(Hz)[6].

Following the lasers are Bragg-cells that are used to modulate the optical frequency, and temperature-stabilized AOTFs for providing the heterodyne frequencies. The optical frequency modulation is a 100 Hz triangle pattern with an amplitude of 86 MHz. The frequency modulation changes the number of optical waves in the shortest metrology beam (3.6 m round-trip) by one wave. This is used to perform cyclic averaging[4] to reduce to acceptable levels the non-linearities arising from polarization leakage in the beam launchers. The heterodyne frequencies used are 100 kHz and 10 kHz for the two lasers, respectively.

Laser light is distributed through single-mode polarization-maintaining (SM/PM) single-mode fiber and a bank of 2 x 8 and 2x2 SM/PM couplers. The couplers reside in the vacuum chamber where temperature stabilities better than 1° C are expected. The fibers and couplers are fusion-spliced to one another; there are no connectors in the system except at the fiber end-points.

The fibers are connected to beam launchers. Beam launchers combine the two incoming polarizations, each at a slightly different frequency, into one beam at a polarizing beam splitter (PBS). Part of the beam is picked off by an R=20% beam splitter and focussed on a detector referred to as the "reference" photo-diode. The phase of the signal on this detector calibrates the optical path fluctuations along the two fibers. The remainder of the beam propagates to a second PBS where one polarization is passed while the other begins a round trip to the corner cubes. The light is recombined at the PBS and is finally focussed on the "unknown" detector. The phase of this signal contains the cumulative optical path difference between the two corner cubes plus the phase difference along the two fibers. The difference between the unknown and reference detector signals yields the round-trip optical path between the corner cubes.

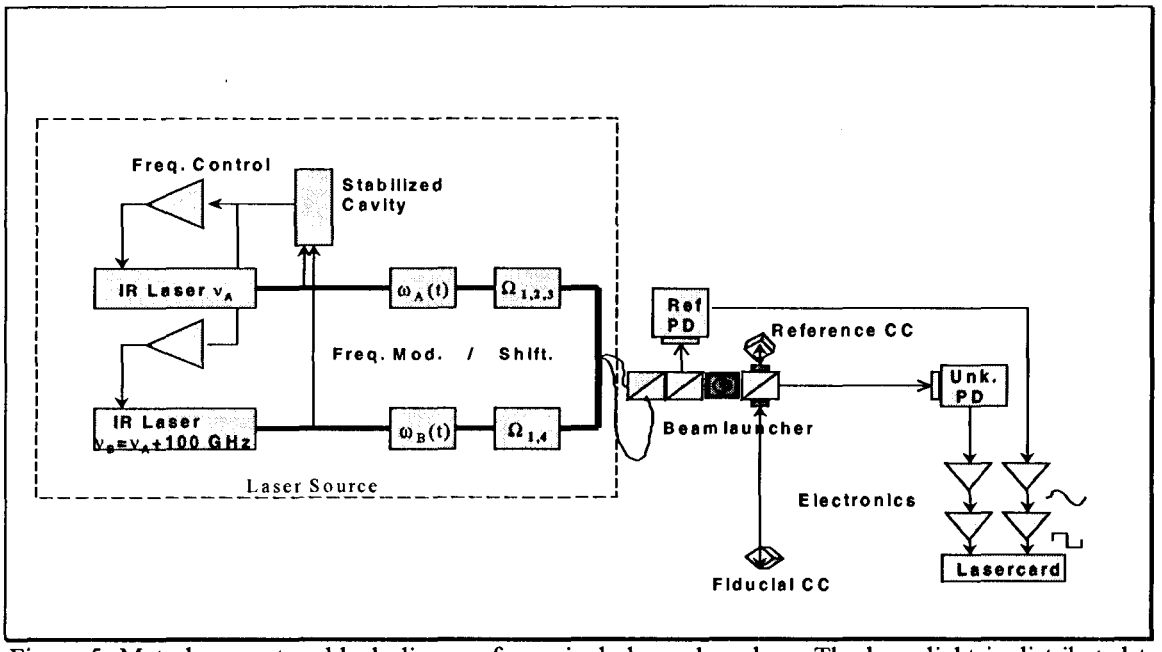

Figure 5. Metrology system block diagram for a single beam launcher. The laser light is distributed to 9 beam launchers. There are 3 laser cards.

The beam launchers are mounted on 3-axis PZT tip-tilt-piston stages. The stages allow a gross alignment of ~ 600 micro-radians. They are used to perform a pointing dither[7] for closed-loop vertex tracking. This is important because pointing errors lead to optical path errors (by the cosine of the pointing error) and additional noise due to imperfections in the optics. We are currently considering multiple-point dithering algorithms as well as modulation/demodulation schemes.

A JPL-designed digital phase meter card ("the laser card") computes the phase difference between the reference and unknown beams. It operates on a 128 MHz clock, detecting a fractional phase with quantization levels of $\lambda/1280 \sim 1$ nm for the 100 kHz signal. The laser card has programmable integration times that allow it to compute the average optical path error as the laser frequency is scanned over 1 wave. This provides not only a means of reducing the cyclic errors (see above), but also averages the quantization noise by a factor of 100-1000.

The end points of the metrology beams are retroreflectors. The central retroreflectors that form the baseline of the 2-D metrology "truss" are triple corner cubes (TCCs); these are three right-angle cubes formed by assembling four ULE prisms[5]. An important feature of the TCC is that the vertices of the three corner cubes are co-located to within 2 microns. Because the vertices are in close proximity to one another, metrology measurements are insensitive to rotations and translations of the TCC. Schmidtlin *et al*[5] describe the construction technique and a our first TCC.

There are also corner cubes located at the centers of the siderostat mirrors. These cubes are constructed in such a way that expansion of the bonding cement does not induce a vertex motion relative to the siderostat surface[2].

The final retroreflector in MAM is a cat's eye formed by a parabola and dichroic mirror at one output of the interferometer (see below). The dichroic reflects the 1.3 micron internal metrology beam while passing the visible starlight beam into a fiber mounted just 500 microns behind the coated surface. The other end of the fiber is connected to the APD.

4.5 Interferometer

The interferometer layout is shown in fig. 6. Light from the artificial star is reflected by a spherical siderostat that has a center-mounted corner cube. The focal length of the siderostat mirror is equal to the nominal distance of the star. This collimates the beam, albeit with a slight amount (about 1/10 wave) of astigmatism. The "cross-eyed" nature of the design forces the astigmatism terms in the two arms to be rotated with respect to one-another. Thus cancellation of the aberration in

the combined beams is not achieved. This places tight constraints on beam alignment as well as optical calibration and modeling.

The clear aperture of the beam is 4.8 cm, with a 14 mm diameter hole for internal metrology. The collimated beam is reflected to a fast-steering mirror (FSM) mounted on a PZT tip-tilt stage. The beam is reflected to delay-line input mirrors that direct it into the delay line. Note the asymmetry of the input mirrors (fig. 6) in the two arms; this corrects the beam and polarization orientation at the interferometer beamsplitter.

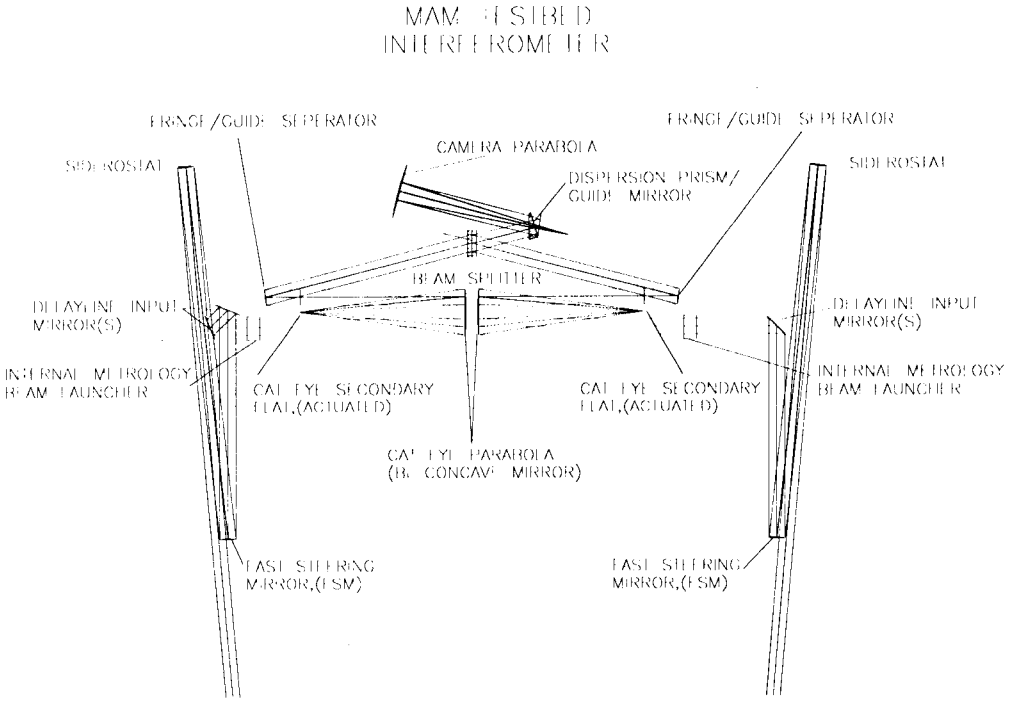

Figure 6. Scale version of interferometer layout. The artificial star is located at the intersection of the two converging lines.

The delay line uses a dual parabola as the primary in both beams. The parabola is formed in the central 6 inches of a 7 inch plane parallel window. The two sides of the window are parallel to 2 arcseconds. These serve as reference planes against which the parabolic axis is measured. The two parabolas are co-axial to an angle of 30 arcseconds. Axial motion of the delay line by a distance d causes a change in optical path difference of 4d. The total delay line motion for a 5 degree motion of the star is ~2 inches.

The delay line secondary mirrors are highly polished (5/2 scratch-dig) flats mounted on momentum-compensated PZT actuators. The secondary of one arm is used to correct optical path fluctuations while the other scans the path to produce a fringe pattern on the APD.

Following the delay line are pairs of optics that separate the angle-tracking light from the fringe light. A dichroic mirror on the first surface of a window reflects the light above 600 nm and passes the shorter wavelengths. The red light is used for fringes and is combined co-axially with the red light from the other arm. The blue light reflects from a mirror that is slightly tilted with respect to the first surface. Each arm has a different, tunable tilt for positioning the guiding spots on the CCD camera.

After combining the beams at a broad-band dielectric sandwich beam splitter, the red beams in the CCD arm are dispersed by a prism/mirror system. The double-pass fused-silica prism achieves a dispersion that is highly uniform in wave-number while directing the central wavelength to be roughly parallel to the blue guide light that reflected from its front surface.

A 47 cm focal length parabola then focuses the beam on a CCD camera (fig. 7). Fringes are seen in the dispersed spectrum with adjacent guide spots. The guide spots are formed at f/10 with a full-width at half-maximum of ~5 microns. This is smaller than the 10 micron pixel size; thus it is crucial for accurate guiding that the spots be positioned on the corners of 4 pixels. This is facilitated by PZT actuators on the fringe/guide separator mirrors.

The beam on the other side of the beamsplitter is reflected from a similar parabola and is focused on the dielectric mirror and fiber optic described in sect. 4.4 above. Details of the interferometer optics can be found in Carlson *et al*[2].

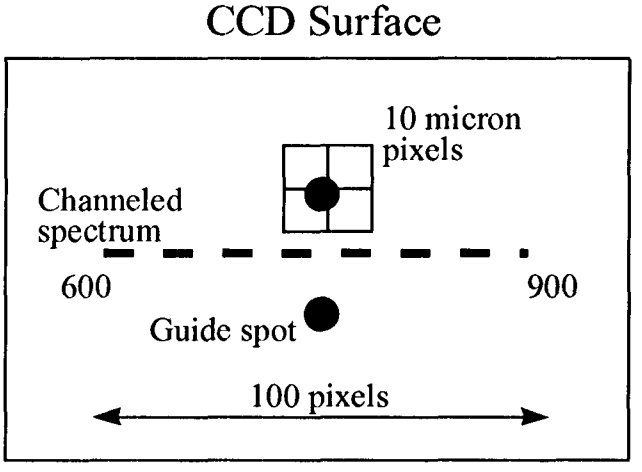

Figure 7. Channeled spectrum and guide spots appearing on the CCD detector.

4.6 Real-time Computer System

The MAM experiment will be controlled by a computer system running on (1) a Sun "UltraSparc" workstation and (2) a VME crate with dual 200 MHz Power-PC 604 CPUs each with 64 Mb of RAM. This system will also collect the data. Communication between the CPUs is handled by two 100 Mbps Ethernet links that connect the Sun system to the two Power-PCs in the VME crate and a 16 MB shared memory card on the VME bus which permits the Power-PCs to communicate with each other .

The VME system incorporates analog and digital interfaces whose functions are (1) data acquisition, (2) control and (3) support, as listed below:

1) VME Boards: Data Acquisition

Integrating laser metrology:

These three laser cards, designed by the JPL, each handle six "reference/unknown" signal pairs from the metrology beam launchers. The processing of these data (by the Power-PC CPUs) is described by Kuhnert et al[4].

Thermal monitoring, misc. analog levels:

This will be handled by three Acromag IP320, 40-channel, 12-bit, "industry pack" modules. (One VME slot can accommodate up to four modules via standard carrier boards.) We plan to monitor temperatures at 100 points distributed throughout the test bed and electronics to characterize sensitivities to temperature fluctuations.

"Starlight" fringe imaging, siderostat guide spot monitoring:

The fringe/guide spots are imaged on a CCD camera that will be read out with a Matrox VIP-640A, 1024x1024 pixels, 8 bit, video card. To preserve bandwidth, only selected regions of the CCD will be readout at the 30 Hz refresh: a 100 x 5 pixel region for the fringes and two 5 x 5 pixel regions for the guide spots.

"Starlight" fringe acquisition and scanning:
In addition to projecting the fringes on a CCD, instantaneous fringe intensity will be monitored with an EG&G APD with a maximum photon flux rate of 10^7 s^{-1}. The APD outputs pulses (one per detected photon) which will be counted by a Greenspring IP-Quadrature "industry pack" module.

Tip-tilt pointing of the two siderostats:
will be monitored to 0.04 micro-radian precision by four MicroE model 5T18 encoders (one per axis). These will be read out by two MicroE DSP interpolator boards (one board per two axis pair). These will present the current position as a 32 bit parallel word that will be read out by two Acromag IP408, 32 bit digital I/O "industry pack" modules.

2) VME Boards: Control

PZT actuation:
For the purposes of metrology beam launcher steering, optic alignment, high-bandwidth star tracking, and high-bandwidth optical delay line control, there will be three Greenspring IP-DAC SU, 16 channel, 16 bit, "industry pack" modules. The output of these modules will be amplified to a 0-100 volt range by custom amplifiers incorporating low-pass filters that will smooth the piezo motions. Each of the nine beam launchers is steered by three PZTs; optical alignment of the two fringe/guide spot separator wedges is adjusted by two PZTs per wedge; the siderostats' motorized star tracking is augmented by two fast steering mirrors with three PZTs per FSM; the two delay line secondary mirrors each incorporate one PZT for piston.

Motor control:
To move the artificial star two Aerotech motors actuated by a Unidex 511 Motion Controller will be used. One of the VME bus Power-PC CPUs will issue motion commands to the motion controller via an auxiliary RS-232 port. Step sizes of 0.1 micron are possible.

For adjusting coarse metrology beam launcher alignment, metrology corner-cube positioning, siderostat steering and coarse delay-line motion, a total of 30 Oriel motors controlled by an Oriel Model 18011 Controller will be used. Because the controller is capable of controlling only three motors, a bank of computer-controlled relays is used to multiplex its output connections. The relays will be actuated by 4 bits of an Acromag IP408, 32 bit digital I/O "industry pack" module, with suitable decoding and buffering to drive the relays.

3) Control

Precision timing
To maintain precise synchronization between the disparate dither, modulation, and metrology readout loops in this system, a custom 32 channel arbitrary programmable frequency VME clock board has been developed. Since each frequency is derived from a common 16 MHz clock which is derived from the same 128 MHz clock that drives the integrating laser metrology cards, overall system synchronization is possible.

4.7 Software

The Real-time Interferometer Control System Testbed (RICST) group at JPL is currently developing software for interferometers that will be used by the various interferometry efforts at JPL including the Mt. Palomar and Keck interferometers, the STB-3 Testbed, DS-3, as well as MAM[8].

The RICST software has two components: a real-time control and monitoring system running on the VME Power-PC CPUs; and a user-interface task running on the Sun workstation. Currently, RICST software can acquire and track "starlight" fringes. Additional efforts are underway to include the metrology, star tracking and miscellaneous monitoring functions needed by MAM and other customers.

Since the RICST software "telemetry" functions have not yet evolved to the level needed by MAM's diagnostic and data recording needs, a commercial software package, "StethoScope" by Real-Time Innovations, Inc., will be used. This software has two components: a data accumulation task running on the VME system, and a graphical display task running on the Sun workstation which will allow real-time display and recording of the value of any variable in the real-time system software.

5. FUTURE WORK

Recently a new configuration has been chosen for the SIM instrument. The new SIM design eliminates siderostats and the external metrology truss and introduces baselines that share a common end-point. The end points are TCCs as described

above. The pointing mechanism, formerly a gimbal in the previous design, is now a hexapod that moves the beam compressors on spherical paths centered on the TCC vertex.

A new configuration for MAM is under consideration. The MAM gimbaled siderostats and siderostat-mounted corner cubes would be replaced with moving beam compressors mounted on a rotation stage with a TCC held above the axis of rotation (but not connected to the stage). The central metrology truss would be eliminated; in its place would go two metrology beams that measure the distance between the artificial star and the TCCs. These would calibrate the external distance to the star. The remainder of the interferometer would go unchanged. The new configuration would better serve the SIM mission by measuring error terms related to beam compressor and TCC alignment. The current plan, however, is to proceed with the existing design to shake out the system and begin characterizing the testbed as soon as possible.

6. ACKNOWLEDGEMENTS

This research was carried out at the Jet Propulsion Laboratory, California Institute of Technology, under a contract with the National Aeronautics and Space Administration. We have received many helpful contributions from Jeffrey Yu, Mike Shao, Feng Zhao, and Bill Harris.

7. REFERENCES

1. S. Unwin, A. Boden, "Science goals of the space interferometry mission," *Proceedings of SPIE Conf. on Astronomical Interferometry*, ed. R. Reasenberg , Vol. 3350, Kona, 1998.
2. A. Carlson, S. Shaklan, S. Azevedo, "Optomechanical design of the micro-arcsecond metrology testbed interferometer," *Proceedings of SPIE Conf. on Astronomical Interferometry*, ed. R. Reasenberg , Vol. 3350, Kona, 1998.
3. S. Dubovitsky, D. Seidel, D. Liu, R. Gutierrez, "Metrology source for high-resolution heterodyne interferometer laser gauges," *Proceedings of SPIE Conf. on Astronomical Interferometry*, ed. R. Reasenberg , Vol. 3350, Kona, 1998.
4. A. Kuhnert, S. Shaklan, Y. Gursel, S. Azevedo, Y. Lin, "Metrology system for the micro-arcsecond metrology testbed," *Proceedings of SPIE Conf. on Astronomical Interferometry*, ed. R. Reasenberg , Vol. 3350, Kona, 1998.
5. E. Schmidtlin, S. Shaklan, A. Carlson, "Novel wide field-of-view laser retroreflectors for the Space Interferometry Mission," *Proceedings of SPIE Conf. on Astronomical Interferometry*, ed. R. Reasenberg , Vol. 3350, Kona, 1998.
6. S. Dubovitsky and D.J. Seidel, "Metrology source frequency stability requirement," JPL IOM 346-96-001 (1996).
7. Y. Gursel, "Metrology for space interferometry V," *Proceedings of SPIE Conf. on Astronomical Interferometry*, ed. R. Reasenberg , Vol. 3350, Kona, 1998.
8. R. Johnson, E. McKenney, D. Slye, K. Starr, "Real-time control software for optical interferometers: the RICST testbed," *Proceedings of SPIE Conf. on Astronomical Interferometry*, ed. R. Reasenberg , Vol. 3350, Kona, 1998.